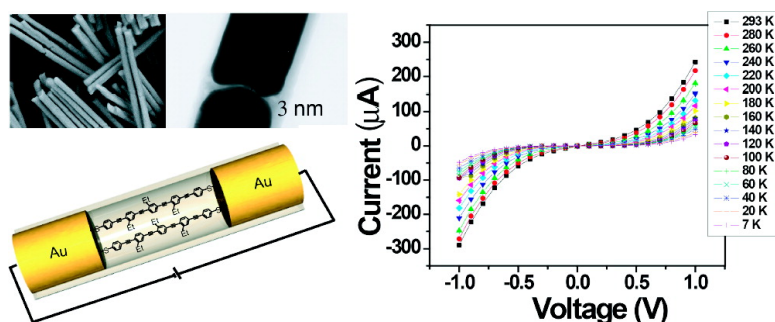


On-Wire Lithography-Generated Molecule-Based Transport Junctions: A New Testbed for Molecular Electronics

Xiaodong Chen, You-Moon Jeon, Jae-Won Jang, Lidong Qin, Fengwei Huo, Wei Wei, and Chad A. Mirkin

J. Am. Chem. Soc., **2008**, 130 (26), 8166-8168 • DOI: 10.1021/ja800338w • Publication Date (Web): 04 June 2008

Downloaded from <http://pubs.acs.org> on February 8, 2009



More About This Article

Additional resources and features associated with this article are available within the HTML version:

- Supporting Information
- Links to the 3 articles that cite this article, as of the time of this article download
- Access to high resolution figures
- Links to articles and content related to this article
- Copyright permission to reproduce figures and/or text from this article

[View the Full Text HTML](#)



On-Wire Lithography-Generated Molecule-Based Transport Junctions: A New Testbed for Molecular Electronics

Xiaodong Chen, You-Moon Jeon, Jae-Won Jang, Lidong Qin, Fengwei Huo, Wei Wei, and Chad A. Mirkin*

Department of Chemistry and International Institute for Nanotechnology, Northwestern University, 2145 Sheridan Road, Evanston, Illinois 60208

Received January 15, 2008; E-mail: chadnano@northwestern.edu

Molecular transport junctions (MTJs) are essential structures for developing the field of molecular electronics.^{1–3} Several techniques have been developed to form such junctions, including ones based upon nanopores,⁴ scanning probes,^{5–7} Hg drop top contacts,⁸ wire crossings,⁹ and template-synthesized materials.¹⁰ All of these techniques can be classified as sequential approaches: the molecules are first covalently attached to one electrode and then a second electrode is brought into contact with the molecules or molecular layers by either mechanical control or metal evaporation. Alternatively, one-step methods for directly assembling molecules into predefined nanogap electrodes have been developed for constructing MTJs. With these one-step approaches, nanogaps have been fabricated by shadow mask evaporation,¹¹ mechanical break junction techniques,^{12,13} electroplating,¹⁴ local oxidative cutting of carbon nanotubes,¹⁵ and electromigration.¹⁶ Although researchers have used these techniques to make impressive advances in measuring the conductance of MTJs,^{5–15} the question of how to reliably fabricate nanogaps between electrodes with the appropriate molecular dimensions in a controlled, high-throughput, and scalable manner remains open.

Recently, we developed an on-wire lithography (OWL)¹⁷ technique to fabricate free-standing nanogaps (Figure 1a and b). The gaps in these systems can be scaled down to ~ 2 nm in a high-throughput and highly reproducible fashion.¹⁸ OWL relies on the template-directed synthesis of nanorods in an anodized aluminum oxide membrane (pore diameter ~ 360 nm) by the electrochemical deposition of desired materials.^{19,20} By selectively introducing a thin sacrificial layer of Ni, one can subsequently create a gap of well-defined thickness by selective wet-chemical etching. The gap size is controlled by the number of coulombs passed in the electrochemical synthesis of the Ni layer. For instance, 3 nm Ni segments are obtained when 30 mC of charge is applied during electrochemical deposition, while 2 nm thick segments result from 20 mC of passed charge. The structure is held together by a thin coat of silica on one face of the wire, which is introduced prior to the etching step. Herein, we demonstrate how OWL-fabricated nanogaps can serve as a new testbed to construct MTJs through the assembly of thiolated molecular wires across a gap formed between two Au electrodes. We show how one can use OWL to easily characterize a MTJ system and optimize gap size for two molecular wires of different dimensions.

In a typical experiment, 360 nm diameter wire structures with ~ 3 nm nanogaps were cast onto a substrate with gold microelectrodes and then connected to the electrodes by e-beam lithography and subsequent chromium and gold thermal deposition (Figure 1c). The unmodified nanogap device was immersed in a tetrahydrofuran (THF) solution of α,ω -dithiol terminated oligo(phenylene ethy-

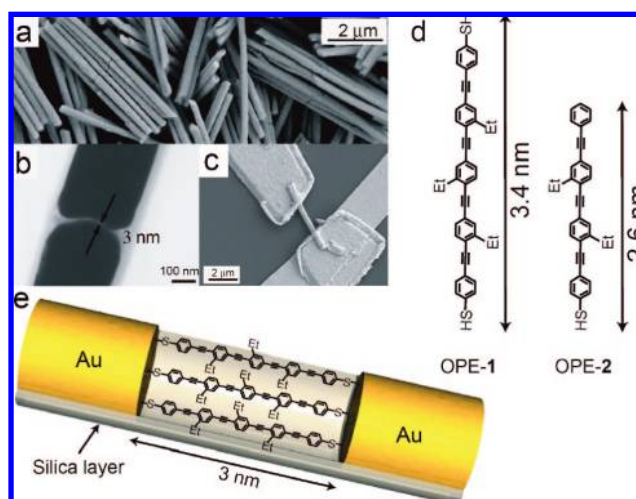


Figure 1. (a) SEM image and (b) TEM image of wires with 3.2 ± 0.4 nm gaps fabricated by OWL; (c) SEM image of a device prepared with an OWL-fabricated wire with a ~ 3 nm gap; (d) molecular structure of OPE-1 and OPE-2; (e) a diagram of OPE-1 molecules spanning the ~ 3 nm gap.

nylene) (OPE-1, ~ 0.2 mg/mL) for 24 h, rinsed with THF, dichloromethane, and ethanol, and then blown dry with N_2 . OPE-1 was selected as a molecular wire because its length is appropriate to span the 3 nm gap defined by the OWL process, and the oligo(phenylene ethynylene) moiety is a well-known, conductive π -conjugated organic molecular wire from which a high quality monolayer can be prepared.²¹

The two terminal I – V characteristics of the ~ 3 nm gap devices were measured at room temperature before and after molecular assembly (Figure 2a). The empty nanogap (black trace, Figure 2a) exhibits no conductance within the noise limit of the measurement (< 2 pA). However, the nanogap devices loaded with OPE-1 show a significant I – V response (red curve, Figure 2a), suggesting the assembly of the molecules across the gap with chemical connectivity to each of the gold electrodes on opposite sides of the gap. Consistent with this conclusion, ~ 3 nm gap devices loaded with a monothiol terminated OPE (OPE-2, Figure 1d) did not exhibit significant current transport across this sized nanogap (red curve, Figure 2b). In addition, 1-octadecanethiol (ODT), 1,16-hexadecanedithiol (HDT), and biphenyl-4,4'-dithiol (BPDT) assembled in such ~ 3 nm gap devices all lead to I – V characteristics similar to open gap structures (Figure 2b). Taken together, these data strongly suggest OPE-1 assembles on the gold nanowires and spans the gap in such a way that it can chemically bond to each of the gold

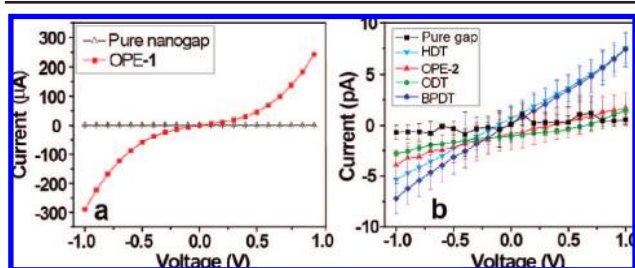


Figure 2. (a) Representative I – V response for ~ 3 nm OWL-fabricated gaps before (black curve) and after (red curve) being modified with OPE-1. (b) I – V response of a ~ 3 nm pure nanogap before (black curve) and after OPE-2, HDT, ODT, and BPDT modification.

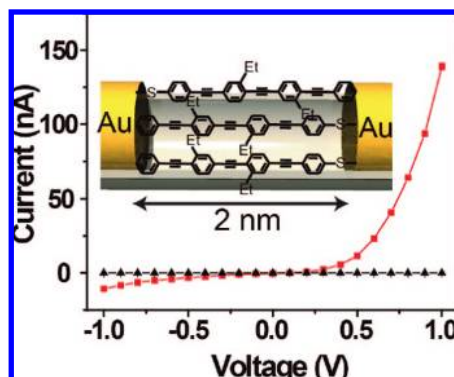


Figure 3. Representative I – V response for 2 nm OWL-fabricated gaps before (black curve) and after (red curve) being modified with OPE-2. (Inset) A diagram of OPE-2 spanning the 2 nm gap in a nanowire fabricated by OWL.

electrodes that are on opposite sides of the gap. It should be noted that the magnitude of the current measured with different devices is different (from 0.1 nA to 300 μ A with 1 V bias), which is presumably due to the number of molecules that actually span the nanogap and make contact with the gold segments (Supporting Information). The roughness of the electrode surface likely contributes to the observed variation.

Significantly, the nanogap size can be rapidly tailored to match the size of a given molecular wire. For instance, when OPE-2 with the length of ~ 2.6 nm is assembled within ~ 2 nm gaps fabricated by OWL, an MTJ is established and rectifying behavior is observed (Figure 3). The rectifying behavior is likely a result of the different modes of contact between the different ends of the molecules and the gold electrodes that span the gap. One end can chemisorb to the electrode while the other is limited to physical contact (Figure 3, inset). These two different metal–molecule contacts induce different electronic coupling of the interface, different injection barriers and unequal voltage drops.^{22–24} For different devices, the current magnitude varies (from 0.07 to 400 nA with 1 V bias), but the rectifying behavior is always observed with this size gap with OPE-2 (Supporting Information). It also should be noted that the rectification ratio, which is defined as the forward current divided by the reverse current, is different in each gap device. This observation may be related to the different possible orientations of OPE-2 within the gap due to its dissymmetric molecular structure (Figure 3, inset). Finally, the rectifying response may imply that the molecules do not create structures with a 1:1 ratio of the two different possible general orientations (determined by the electrode to which thiol adsorption occurs). This could be due to templated

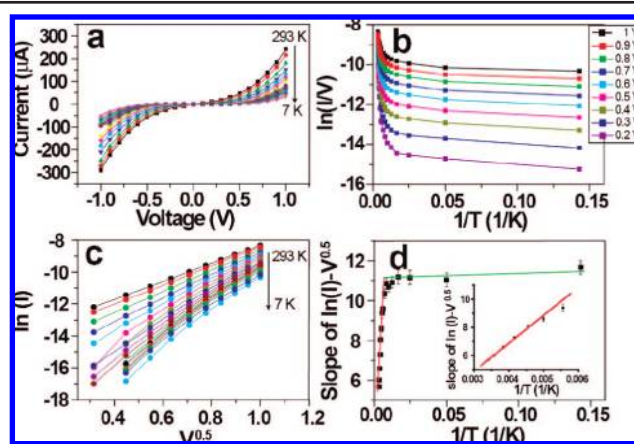


Figure 4. (a) Temperature dependent I – V response of OPE-1 bridging the 3 nm nanogap fabricated by OWL. (b) Plots of $\ln(I/V)$ as a function of $1/T$ for different biases. (c) Plots of $\ln(I)$ vs $V^{0.5}$ with biases from 0.1 to 1.0 V at different temperature. (d) Plot of the slope of $\ln(I) - V^{0.5}$ vs $1/T$. The inset shows the magnification of the high temperature part with linear fitting. All of the straight lines are χ^2 fits for respective data sets.

assembly, where the initial adsorption event directs subsequent events to create structures with a predominance of one orientation.

These new MTJs not only provide a rapid way of matching gap size and electrode composition with molecular electronic components of interest (note, we have made electrodes out of Au, Pt, Pd and Ag thus far),¹⁷ but also allow one to rapidly define the intrinsic transport properties of the molecules that span the gaps. For example, we studied the temperature dependent I – V characteristics of the OPE-1-modified junction (Figure 4a) to elucidate the conduction mechanism of the device. The monotonic decrease of current with temperature suggests a thermally activated transport mechanism, such as thermionic emission or hopping conduction.²⁵ However, hopping conduction can be excluded on the basis of the temperature-dependent voltage dependence.²⁶ When $\ln(I/V)$ is plotted as a function of $1/T$ the curves should be identical for hopping conduction; but instead one sees a clear difference as a function of voltage (Figure 4b). However, if one plots $\ln(I)$ vs $V^{0.5}$, a linear dependence is observed (Figure 4c), which is characteristic of thermionic emission.^{25,27} This dependence comes from the following relationship²⁸

$$I = AT^2 \exp\left(-\frac{q\Phi - q\sqrt{\frac{qV}{4\pi\epsilon_0\epsilon d}}}{kT}\right) \quad (1)$$

where A is the effective Richardson constant multiplied by the current injection area, Φ is the thermal emission barrier height, k is the Boltzmann's constant, q is the electron charge, ϵ_0 is the vacuum dielectric constant, ϵ is the relative dielectric constant of the OPE-1 layer, and d is the thickness of the OPE-1 monolayer.

It is important to note that the disordered film model, which describes charge injection from a metal into a disordered organic film, predicts a current–voltage dependence similar to the thermionic emission model.^{29–31} This model is often used to describe charge injection in light emitting diodes (LEDs), which have disordered multilayers of organic molecules between the metal electrodes in the device. We use the thermionic emission model to describe our system because the monolayer of OPE-1 molecules are chemisorbed to the electrodes on opposite sides of the gap and

significantly more oriented and ordered than the types of molecules found in conventional LEDs.

At high temperatures (>120 K) (red line, Figure 4d), the response of the MTJ fits well with a thermionic emission mechanism, which involves thermally activated charge injection from the electrode to the OPE-1. From the slope of the line formed from plotting $\ln(I) - V^{0.5}$ as a function of temperature, one can determine the relative dielectric constant of the OPE-1 layer to be 16.4, the thermal barrier height to be 0.19 eV, and the Richardson constant to be 21 A/cm^2 . This assumes a monolayer thickness of 3 nm, the average size of the nanogap. These values are comparable to ones reported for other organic molecular wires.^{26,27} However, at low temperatures (<120 K), charge transport is dominated by tunneling.³² Consistent with this conclusion, the $I-V$ response is minimally dependent upon temperature (green line, Figure 4d). Therefore, there are two different charge transport mechanisms depending on temperature for the OPE-1 MTJs based on the OWL-fabricated nanogaps: at low temperature (>120 K), electrons tunnel across the barrier through the intervening states; as the temperature increases, thermal emission of electrons over a barrier of 0.19 eV dominates electron injection from Au to the OPE-1 layer, thus reducing the contribution from the tunneling process. The transition from tunneling to thermionic emission at high temperature is likely the result of thermal fluctuations and the onset of torsional fluctuations of the phenyl rings in OPE-1. Others have invoked this type of torsional fluctuation to explain transitions between different transport mechanisms.³³ It is worth noting that this is the first experimental observation of a transition from tunneling to thermionic emission in a MTJ, although there are two examples of other kinds of transport transitions: tunneling to hopping (depending on temperature)³⁴ and tunneling to field emission (depending on bias).³⁵ The different transition behaviors suggest the importance of local environment and the means by which molecules are contacted.³⁶

In summary, this work is important for the following reasons. First, it shows how one can use OWL to rapidly construct electrodes with gaps small enough to accommodate “molecular wires”, and that the gap size can be tailored for a given molecule. Second, the process is high-throughput, with respect to gap fabrication, and extremely flexible with respect to the type of materials one can use as an electrode. Anything that can be plated in an electrochemical experiment is an electrode candidate material. Third, the approach allows one to easily study the properties of molecular wires, and we have created an initial testbed to identify unusual transport mechanism differences for one type of molecular wire (OPE-1) as a function of temperature. Indeed, from a molecular electronics point of view, OWL-fabricated structures offer a transport testbed of remarkable simplicity, stability, and scalability. In addition, OWL-fabricated MTJs may be used for a variety of applications that extend beyond electronics, including chemical and biological sensing when more sophisticated molecules are used to make them.

Acknowledgment. CAM acknowledges support from AFOSR, NSF-NSEC, and DARPA. CAM is also grateful for an NIH Director’s Pioneer Award. We thank Professor Mark Ratner for his insight and preliminary review of this manuscript. The authors

also thank Drs. Gengfeng Zheng, Ling Huang, Jacob W. Ciszek, Dwight S. Seferos, Mr. David Giljohann, and Miss Louis Giam for experimental assistance and valuable discussion.

Supporting Information Available: Complete ref 15; experimental procedures including molecule synthesis, device fabrication, and characterization data. This material is available free of charge via the Internet at <http://pubs.acs.org>.

References

- (1) Lindsay, S. M.; Ratner, M. A. *Adv. Mater.* **2007**, *19*, 23–31.
- (2) Nitzan, A.; Ratner, M. A. *Science* **2003**, *300*, 1384–1389.
- (3) Tao, N. J. *Nat. Nano.* **2006**, *1*, 173–181.
- (4) Chen, J.; Reed, M. A.; Rawlett, A. M.; Tour, J. M. *Science* **1999**, *286*, 1550–1552.
- (5) Xu, B. Q.; Tao, N. J. *Science* **2003**, *301*, 1221–1223.
- (6) Cui, X. D.; Primak, A.; Zarate, X.; Tomfohr, J.; Sankey, O. F.; Moore, A. L.; Moore, T. A.; Gust, D.; Harris, G.; Lindsay, S. M. *Science* **2001**, *294*, 571–574.
- (7) Bumm, L. A.; Arnold, J. J.; Cygan, M. T.; Dunbar, T. D.; Burgin, T. P.; Jones, L.; Allara, D. L.; Tour, J. M.; Weiss, P. S. *Science* **1996**, *271*, 1705–1707.
- (8) Holmlin, R. E.; Haag, R.; Chabynyc, M. L.; Ismagilov, R. F.; Cohen, A. E.; Terfort, A.; Rampi, M. A.; Whitesides, G. M. *J. Am. Chem. Soc.* **2001**, *123*, 5075–5085.
- (9) Kushmerick, J. G.; Holt, D. B.; Pollack, S. K.; Ratner, M. A.; Yang, J. C.; Schull, T. L.; Naciri, J.; Moore, M. H.; Shashidhar, R. *J. Am. Chem. Soc.* **2002**, *124*, 10654–10655.
- (10) Mbindyo, J. K. N.; Mallouk, T. E.; Mattzela, J. B.; Kratochvilova, I.; Razavi, B.; Jackson, T. N.; Mayer, T. S. *J. Am. Chem. Soc.* **2002**, *124*, 4020–4026.
- (11) Tang, J. Y.; Wang, Y. L.; Klare, J. E.; Tulevski, G. S.; Wind, S. J.; Nuckolls, C. *Angew. Chem., Int. Ed.* **2007**, *46*, 3892–3895.
- (12) Reed, M. A.; Zhou, C.; Muller, C. J.; Burgin, T. P.; Tour, J. M. *Science* **1997**, *278*, 252–254.
- (13) Reichert, J.; Ochs, R.; Beckmann, D.; Weber, H. B.; Mayor, M.; von Lohneysen, H. *Phys. Rev. Lett.* **2002**, *88*, 176804.
- (14) Hu, W. P.; Nakashima, H.; Furukawa, K.; Kashimura, Y.; Ajito, K.; Liu, Y. Q.; Zhu, D. B.; Torimitsu, K. *J. Am. Chem. Soc.* **2005**, *127*, 2804–2805.
- (15) Guo, X. F.; et al. *Science* **2006**, *311*, 356–359.
- (16) Park, H.; Lim, A. K. L.; Alivisatos, A. P.; Park, J.; McEuen, P. L. *Appl. Phys. Lett.* **1999**, *75*, 301–303.
- (17) Qin, L. D.; Park, S.; Huang, L.; Mirkin, C. A. *Science* **2005**, *309*, 113–115.
- (18) Qin, L. D.; Jang, J. W.; Huang, L.; Mirkin, C. A. *Small* **2007**, *3*, 86–90.
- (19) Hurst, S. J.; Payne, E. K.; Qin, L. D.; Mirkin, C. A. *Angew. Chem., Int. Ed.* **2006**, *45*, 2672–2692.
- (20) Martin, C. R. *Science* **1994**, *266*, 1961–1966.
- (21) Tour, J. M. *Acc. Chem. Res.* **2000**, *33*, 791–804.
- (22) Dhirani, A.; Lin, P. H.; Guyot-Sionnest, P.; Zehner, R. W.; Sita, L. R. *J. Chem. Phys.* **1997**, *106*, 5249–5253.
- (23) Taylor, J.; Brandbyge, M.; Stokbro, K. *Phys. Rev. Lett.* **2002**, *89*, 138301.
- (24) Kushmerick, J. G.; Holt, D. B.; Yang, J. C.; Naciri, J.; Moore, M. H.; Shashidhar, R. *Phys. Rev. Lett.* **2002**, *89*, 086802.
- (25) Wang, W. Y.; Lee, T.; Reed, M. A. *Phys. Rev. B* **2003**, *68*, 035416.
- (26) Zhou, C.; Deshpande, M. R.; Reed, M. A.; Jones, L.; Tour, J. M. *Appl. Phys. Lett.* **1997**, *71*, 611–613.
- (27) Chen, J.; Calvet, L. C.; Reed, M. A.; Carr, D. W.; Grubisha, D. S.; Bennett, D. W. *Chem. Phys. Lett.* **1999**, *313*, 741–748.
- (28) Sze, S. M. *Physics of Semiconductor Devices*; Wiley: New York, 1981; p 403.
- (29) Burin, A. L.; Ratner, M. A. *J. Polym. Sci. B: Polym. Phys.* **2003**, *41*, 2601–2621.
- (30) Barth, S.; Wolf, U.; Bassler, H.; Muller, P.; Riel, H.; Vestweber, H.; Seidler, P. F.; Riess, W. *Phys. Rev. B* **1999**, *60*, 8791–8797.
- (31) Wolf, U.; Arkhipov, V. I.; Bassler, H. *Phys. Rev. B* **1999**, *59*, 7507–7513.
- (32) Segal, D.; Nitzan, A.; Davis, W. B.; Wasielewski, M. R.; Ratner, M. A. *J. Phys. Chem. B* **2000**, *104*, 3817–3829.
- (33) Selzer, Y.; Cai, L. T.; Cabassi, M. A.; Yao, Y. X.; Tour, J. M.; Mayer, T. S.; Allara, D. L. *Nano Lett.* **2005**, *5*, 61–65.
- (34) Selzer, Y.; Cabassi, M. A.; Mayer, T. S.; Allara, D. L. *J. Am. Chem. Soc.* **2004**, *126*, 4052–4053.
- (35) Beebe, J. M.; Kim, B.; Gadzuk, J. W.; Frisbie, C. D.; Kushmerick, J. G. *Phys. Rev. Lett.* **2006**, *97*, 026801.
- (36) Nitzan, A. *Annu. Rev. Phys. Chem.* **2001**, *52*, 681–750.

JA800338W